Efficiency in the Generation of the Boltzmann−Gibbs Distribution by the Tsallis Dynamics Reweighting Method

Ikuo Fukuda*,† and Haruki Nakamura†,‡

National Institute of Advanced Industrial Science and Technology, 2-41-6, Aomi, Koto-ku, Tokyo 135-0064, Japan, and Institute for Protein Research, Osaka University, 3-2 Yamadaoka, Suita, Osaka 565-0871, Japan

Received: September 23, 2003; In Final Form: January 7, 2004

We numerically investigated deterministic methods for constructing the Boltzmann−Gibbs (BG) distributions used in molecular dynamics simulations. Tsallis dynamics (TD) is a deterministic dynamical equation that can generate the Tsallis distribution and reconstruct the BG distributions by a reweighting method. This method is applied to the 1-dimensional harmonic oscillator and 1-dimensional double-well potential, which are fundamental interaction models and have been typical examples yielding problematic results in conventional molecular dynamics simulations. We examined the ability of TD to produce the BG distributions using these low-dimensional models and the alanine tripeptide system, comparing the results with those of a conventional deterministic method that directly produces the BG distribution. We found the TD produced efficient sampling, including full phase-space covering to generate the correct BG distribution for the 1-dimensional harmonic oscillator, powerful barrier crossing against the traps at the local minima of the double-well potential, and a wide-region sampling in the potential energy space for the alanine system. Problems for the method are also discussed.

1. Introduction

Molecular dynamics (MD) simulations have revealed the nature of various physical systems, on the basis of the microscopic atomic descriptions and the deterministic continuous time evolution. The Boltzmann−Gibbs (BG) distribution provides links between the evaluation of thermal quantities obtained by the simulation for the targeted system and the experimental results. In this paper, we focus on the deterministic methods for generating the BG distributions in continuous systems, and we consider how those distributions are effectively constructed. For such methods, two approaches exist: direct and indirect.

BG dynamics (BGD) is described by a deterministic equation that can construct the BG distribution in a direct way (direct approach). BGD for continuous physical systems[1] was developed by Nosé and Hoover.[2,3] The breakthrough caused by the Nosé−Hoover (NH) equation has significantly influenced the MD simulations, and a variety of BGD methods have been proposed[4,5] since the equation was developed. BGD is not limited to the calculation of thermodynamic quantities. For example, it has provided various applications for nonequilibrium physical phenomena and has been used to reveal physical foundations including a relation between microscopic time-reversible dynamics and macroscopic irreversibility.[6] In view of effective sampling of the BG distribution, however, the method has been recognized to have a limited ability to generate the distributions for certain physical systems. One example is a 1-dimensional harmonic oscillator (1HO) system, in which difficulties arise when we derive the required ergodicity in the "extended system" from the regular motions in the original integrable Hamilton system.[7] The Nosé−Hoover chain (NHC) method[8] is one of the promising methods to overcome the problem, and accompanies various applications (see, e.g., refs 9 and 10 and the references therein). Another example is a double-well potential system, which often makes BGD suffer from local traps in conventional simulations. When an accurate BGD is required, a probability $\propto\exp(-\beta E)$ even at a high energy barrier should be provided accurately, where E is the energy for the system. Accordingly, the simulation requires a long time to escape beyond such barriers, as the accuracy is highly increased. It has been indicated that low-dimensional double-well systems do not always lead to correct distributions or expectation values of physical quantities in conventional BGD.[11,12] Obtaining accurate distributions for those systems is important because the harmonic oscillator potential and double-well potential are fundamental atomic interaction models and prototypes of chemical phenomenological potential models.

Indirect approach is to construct a certain distribution that is different from the BG distribution and then to reconstruct the BG distribution. For the reconstruction, the "reweighting" technique proposed in ref 13 can be used. Multicanonical molecular dynamics (MCMD) is a representative method in these indirect approaches.[14] Although these methods have been studied intensively, their efficiency is still limited, particularly for application to large and complex systems.

One of the most important abilities for effective sampling in a given distribution is (i) to sample a high-probability area (i.e., an area to which high probability is distributed) within a given restricted time and (ii) to move into another high-probability area, not staying in a single area, but jumping across low-probability regions as the obstacles to effective sampling. As mentioned above, it is difficult to balance conditions i and ii

* Address correspondence to this author. Fax: +81-3-3599-8099. E-mail: ifukuda@jbirc.aist.go.jp.
† National Institute of Advanced Industrial Science and Technology.
‡ Osaka University.

10.1021/jp031086w CCC: $27.50
Published on Web 03/10/2004

by using the direct approach. When we consider the indirect approach, it is thought to be effectual, from the standpoint of condition i, that the construction of an appropriate distribution that does not deviate much from the given distribution and retains a certain weight at the originally given high-probability area.

One candidate of such distributions near the BG distribution is the Tsallis distribution,[15,16] which may satisfy both conditions i and ii. This distribution is an extension of the BG distribution by one parameter, q, and it converges to the BG distribution as q tends to 1. Furthermore, the value of the Tsallis distribution with $q > 1$ decreases more slowly (power law) as E increases than the BG distribution does (exponential law). This means that high-energy states can be realized more frequently than those in the BG distribution. Thus, we expect high performance in overcoming the energy barriers, avoiding the local traps effectively.

Some deterministic methods have been developed for generating the Tsallis distribution described from total energy (Hamiltonian) defined by both the coordinates and momenta. Plastino and Anteneodo[17] devised such a method, where the applicability is centered on the $q < 1$ region, using the procedure of Kusnezov, Bulgac, and Bauer.[11] In our previous work we proposed Tsallis dynamics (TD),[18] in which the Tsallis-distributed system with $q > 1$ was realized based on the NH method. Andrade et al.[19] have proposed a "Hamiltonian approach" to achieve the Tsallis distribution, in conjunction with Winkler's method.[20]

In this study, to provide the BG distributions by the reweighting procedure in the Tsallis-distributed system constructed by the TD, we examined the abilities of the indirect approach in detail, using several model systems. We performed numerical simulations to calculate the distributions and expectation values for the above stiff low-dimensional systems, and for studies in more realistic problems we applied our method to a system of the alanine tripeptide. We clarify the efficiencies and subjects of this approach by comparing them with those of other methods.

In Section 2, we demonstrate the TD and the reweighting method for realizing the BG distributions. In Section 3.1, we apply the current method to the low-dimensional problems and compare its performance numerically with that of the NHC method. In Section 3.2, the results of application to the alanine tripeptide are shown. Section 4 is devoted to reviewing our conclusions.

2. The Tsallis Dynamics and the Reweighting Method

The Tsallis distribution density, apart from the normalization, has the following form:

$$\rho_{\mathrm{Tsallis}}(x,p) = [1 - (1-q)\beta E(x,p)]^{q/(1-q)} \qquad (1)$$

where E:$\mathbf{R}^{2n} \supset \Gamma \equiv D \times \mathbf{R}^n \to \mathbf{R}$, $(x,p) \to K(p) + U(x)$, $U(x)$ is a potential energy, and $K(p) \equiv {}^1/_2||p||^2 \equiv {}^1/_2\sum_{i=1}^n p_i^2$ is a kinetic energy. Here, $x \equiv (x_1, ..., x_n)$ and $p \equiv (p_1, ..., p_n)$ are the coordinates and the momenta, respectively. The parameter q is called the "Tsallis index", and the density approaches $\rho_{\mathrm{BG}}(x,p) \equiv \exp[-\beta E(x,p)]$ ($\propto$ the density of the BG distribution), as $q \to 1$. We used "escort probabilities" and the "renormalized temperature"[16,21] $T' > 0$ with $\beta \equiv 1/T'$ in eq 1 (we put all masses and the Boltzmann constant, k_{B}, at unity), and assume $q > 1$.

The TD is an ordinary differential equation (ODE), which is based on the Nosé−Hoover method[2,3] and can produce the Tsallis distribution, represented (in T'-multiplied form) by

$$\begin{aligned} \dot{x}_i &= g(x,p)p_i \qquad (i = 1, ..., n) \\ \dot{p}_i &= -g(x,p)D_iU(x) - \tau(\zeta)p_i \qquad (i = 1, ..., n) \\ \dot{\zeta} &= g(x,p)||p||^2 - nT' \end{aligned} \qquad (2)$$

where $g(x,p) \equiv q/[1 - (1-q)\beta E(x,p)]$ and $\tau(\zeta) \equiv -T'(\mathrm{d}/\mathrm{d}\zeta) \ln \rho_z(\zeta)$. The flow generated by this ODE (assuming completeness) has an invariant measure $\rho \mathrm{d}\omega$, where $\rho(x,p,\zeta) \equiv \rho_{\mathrm{Tsallis}}(x,p)\rho_z(\zeta)$, ρ_z:$\mathbf{R} \to \mathbf{R}$, and $\mathrm{d}\omega$ is Lebesgue measure on $\mathbf{R}^{2n+1}$. Assuming a certain condition for ρ, if the flow is ergodic with respect to the measure $\rho \mathrm{d}\omega$, then for any physical quantity A:$\Gamma \to \mathbf{R}$ with the condition of $\int_{\Gamma\times\mathbf{R}}|A\rho|\ \mathrm{d}\omega < +\infty$, and for ($\rho \mathrm{d}\omega$) almost every (a.e.) initial point, the following holds:

$$\begin{aligned} \bar{A} &\equiv \lim_{\tau\to\infty}\frac{1}{\tau}\int_0^\tau A(x(t),p(t))\ \mathrm{d}t \\ &= \int_{\Gamma\times\mathbf{R}} A(x,p)\rho(\omega)\ \mathrm{d}\omega \Big/ \int_{\Gamma\times\mathbf{R}} \rho(\omega)\ \mathrm{d}\omega \\ &= \int_\Gamma A(x,p)\rho_{\mathrm{Tsallis}}(x,p)\ \mathrm{d}x\ \mathrm{d}p \Big/ \int_\Gamma \rho_{\mathrm{Tsallis}}\ \mathrm{d}x\ \mathrm{d}p \end{aligned} \qquad (3)$$

Namely, an expectation of A in the Tsallis distribution is evaluated by the long-time average obtained from eq 2.

The BG distributions are obtained by the following reweighting method. Under the ergodicity with the same assumptions described above, for any physical quantity A, we can prove

$$\begin{aligned} &\overline{A\rho_{\mathrm{BG}}/\rho_{\mathrm{Tsallis}}} \Big/ \overline{\rho_{\mathrm{BG}}/\rho_{\mathrm{Tsallis}}} \\ &\qquad = \int_\Gamma A(x,p)\rho_{\mathrm{BG}}(x,p)\ \mathrm{d}x\ \mathrm{d}p \Big/ \int_\Gamma \rho_{\mathrm{BG}}\ \mathrm{d}x\ \mathrm{d}p\ \text{(a.e.)} \\ &\qquad \equiv \langle A \rangle \end{aligned} \qquad (4)$$

where the space integrals are assumed to be finite. Thus, an expectation of A in the BG distribution can be obtained, when we evaluate the long-time averages for $A\rho_{\mathrm{BG}}/\rho_{\mathrm{Tsallis}}$ and $\rho_{\mathrm{BG}}/\rho_{\mathrm{Tsallis}}$. The reweighting method enables us to generate many BG distributions, each corresponding to $\exp[-E(x,p)/T]$ with an arbitrarily assigned temperature $T > 0$, in a single simulation.

3. Results and Discussion

We carried out numerical simulations to examine the ability of the current method to generate the BG distributions, and compared the results with those of other methods.

3.1. Low-Dimensional Problems. The potential models of 1HO and 1-dimensional double-well (1DW) were treated. We used the 4th-order Runge−Kutta method for the integration of the ODEs. All variables were treated as dimensionless. In the current method, a simulated value of the expectation in the BG distribution for quantity A was evaluated from the finite-time value of the left-hand side of eq 4:

$$\bar{A}^{\mathrm{BG},t} \equiv \int_{t_0}^t (A\rho_d)(x(s),p(s))\ \mathrm{d}s \Big/ \int_{t_0}^t \rho_d(x(s),p(s))\ \mathrm{d}s \qquad (5)$$

Here, $\rho_d \equiv \rho_{\mathrm{BG}}/\rho_{\mathrm{Tsallis}}$; $t_0 \equiv N_0\Delta t$ was chosen to be sufficiently smaller than the total time $t = t_T$, Δt being a unit time step. To examine the correctness of the obtained BG distribution, we calculated each component, i.e., the marginal distribution density (MDD). The MDD with respect to a variable ω_i, f_i, is defined by $f_i(\omega_i) \equiv \int_{\mathbf{R}^{2n-1}} \mathrm{d}\omega_1 \cdots \mathrm{d}\omega_{i-1}\ \mathrm{d}\omega_{i+1} \cdots \mathrm{d}\omega_{2n}\rho_{\mathrm{BG}}(\omega_1, ..., \omega_{2n}) / \int_{\mathbf{R}^{2n}} \mathrm{d}x\ \mathrm{d}p\ \rho_{\mathrm{BG}}$. In our 1-dimensional case, we can represent this value for $i = 1$ as $f_1(\bar{x}) = \int_{\mathbf{R}} \mathrm{d}p\ \rho_{\mathrm{BG}}(\bar{x},p) / \int_{\mathbf{R}^2} \mathrm{d}x\ \mathrm{d}p\ \rho_{\mathrm{BG}}(x,p)$

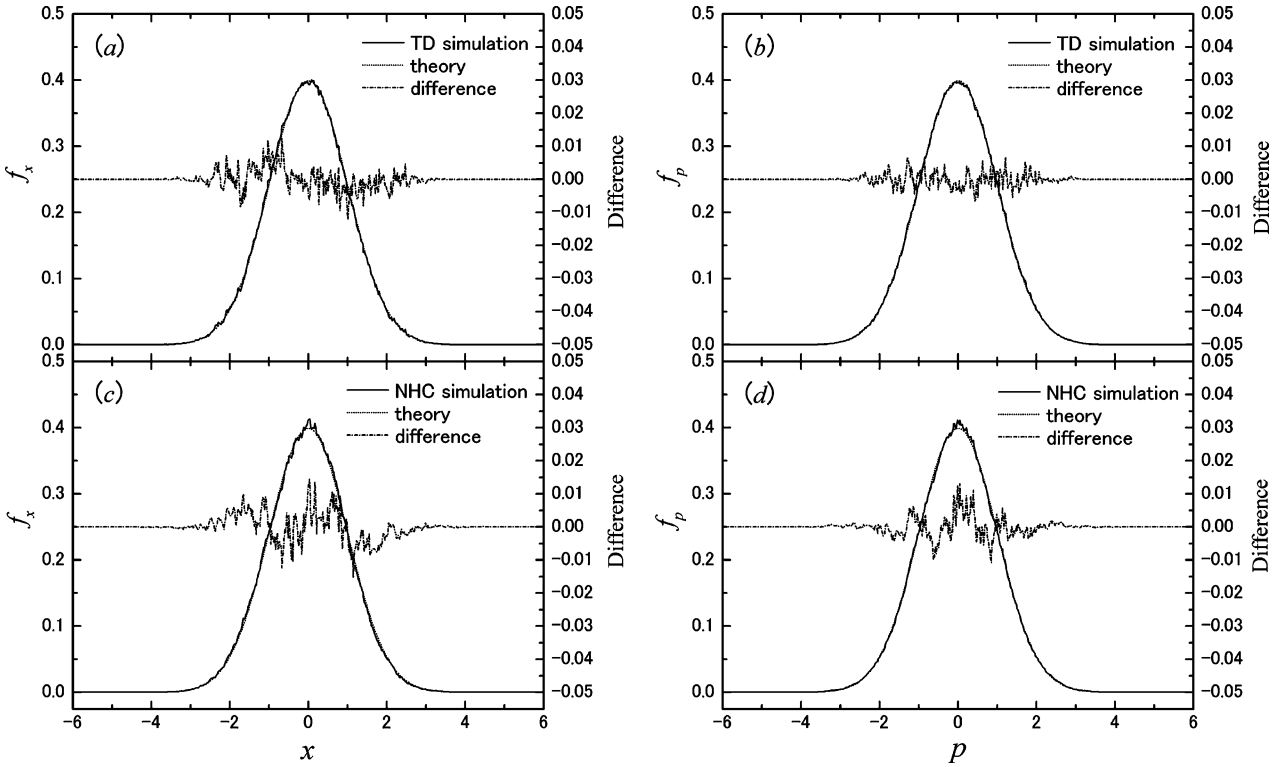

Figure 1. MDD of 1HO for component of (a) x and (b) p. The solid and dotted lines indicate simulation results obtained by the TD method and the theoretical values, respectively. The difference indicating the former minus the latter is shown at an enlarged scale by the dash−dotted line. Simulation results of the MDD obtained by the NHC method, the theoretical values, and their differences are shown for (c) x and (d) p.

$\simeq \int_{\mathbf{R}^2} \mathrm{d}x\, \mathrm{d}p\, |\bar{I}_1|^{-1}\chi_{\bar{I}_1}(x,p)\rho_{\mathrm{BG}}(x,p)/\int_{\mathbf{R}^2} \mathrm{d}x\, \mathrm{d}p\, \rho_{\mathrm{BG}}$. Here $\bar{x}$ is supposed to be contained in a bin $\bar{I}_1 \subset \mathbf{R}$, $|\bar{I}_1|$ is the bin size assumed to be sufficiently small, and $\chi_{\bar{I}_1}$ is the characteristic function for $\bar{I}_1$, which takes a value of 1 if $x \in \bar{I}_1$ and takes 0 otherwise. A similar expression holds for f_2, and we denote that $f_x \equiv f_1$ and $f_p \equiv f_2$. The simulated value of the MDD for the ith component was thus evaluated piecewise, i.e., letting $A \equiv |I_{i,\nu}|^{-1}\chi_{I_{i,\nu}}$ in eq 5 (ρ_d is replaced by 1 in the BGD case) for each bin indexed by $\nu \in \mathbf{Z}$. A total error of MDD at time t was estimated from $\Delta_i(t) \equiv ||f_i^t - f_i||_1 \equiv \int_{\mathbf{R}} |f_i^t(\omega_i) - f_i(\omega_i)|\, \mathrm{d}\omega_i \in [0,2]$. Here, $f_i^t(\omega_i)$ is the simulated MDD value evaluated up to time t from t_0, satisfying $||f_i^t||_1 = ||f_i||_1 = 1$. In all results, the following conditions were used: temperature parameters, $T = T' = 1$; Tsallis index, $q = 3$; and $N_0 = 10^4$. An initial value for the ODE was $x(0) = 0$, $p(0) = 1$, and $\zeta(0) = 0$, unless stated. The sizes of bins were $|I_{1,\nu}| = |I_{2,\nu}| = 0.02$ for all ν.

3.1.1. One-Dimensional Harmonic Oscillator. The TD simulation for the 1HO,

$$U(x) = \frac{1}{2}x^2 \tag{6}$$

was performed. Panels a and b in Figure 1 show the MDDs obtained for $N = 10^7$ time steps with $\Delta t = 5 \times 10^{-3}$ and for $\tau(\zeta) = 100\zeta^3$ (eq 2). The differences $f_i^{N\Delta t}(\omega_i) - f_i(\omega_i)$ are also shown. Simulation results for the MDDs agreed with the theoretical one with very small differences. For comparison, we applied the same potential to the NHC method. As in ref 8, the "chain length" of $M = 2$ was used, the initial values of the "thermostat momenta" were $p_{\eta_1}(0) = p_{\eta_2}(0) = 1$, and their corresponding "thermostat masses" were $Q_1 = Q_2 = 1$. Other conditions were the same as for the TD. We verified the agreement between the simulated results for the NHC and the theoretical values, which resulted in a similar accuracy to that in the TD, as indicated in Figure 1, panels c and d.

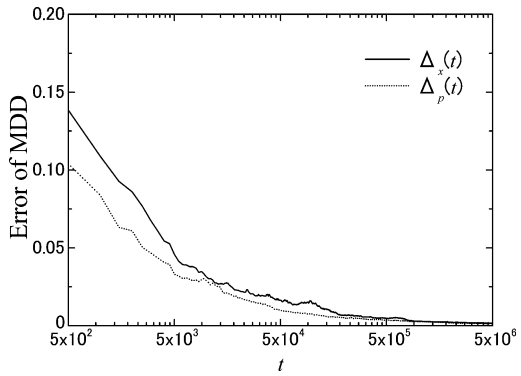

Figure 2. The total error of MDD vs time t for 1HO, obtained by TD. The solid and dotted lines indicate the errors for components of x, $\Delta_x(t)$, and of p, $\Delta_p(t)$, respectively.

A total error of MDD obtained by the current TD method, $\Delta_i(t)$, is shown until $t = N\Delta t = 5 \times 10^6$ (Figure 2). Convergence can be observed. To examine the initial condition dependency for the TD, we carried out simulations for a number of initial values chosen randomly within $|x| \leq 3$, $|p| \leq 3$, and $|\zeta| \leq 1$, and similar results were obtained.

Thus, when we use eq 2, which is a q-deformed equation[18] of the NH equation, together with a suitable choice of $\tau(\zeta)$, and when we recover the BG distribution ($q = 1$) by the reweighting, we can generate the BG distribution for 1HO. By increasing the number of thermostats and their coupling, the NHC method has improved the ability to obtain ergodicity in the extended system, even for a simple given system, such as 1HO. In contrast, in the current TD, having sufficiently nonlinear features in the equation could increase the ability to attain the ergodicity.

Concerning the choice for $\tau(\zeta)$, we have varied the values of c in $\tau(\zeta) = c\zeta^3$, as $c = 10$, 50, 500, and 1000. The MDD errors all tended to be small values ($\lesssim 0.01$ at $N = 10^8$ time steps).

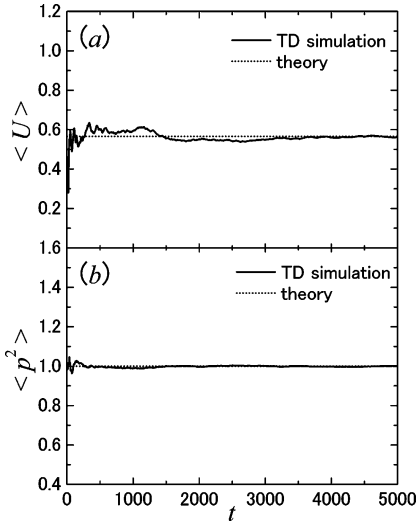

Figure 3. Expectation value of (a) U and (b) p^2 for 1DW with $D = 5k_BT$. Simulation results by TD evaluated up to time t vs t are shown by solid lines. The dotted lines indicate the theoretical values.

Although good results similar to those described above were also obtained in the case of $\tau(\zeta) = c\zeta$ for a specific value of c (e.g., $c = 10$), the third-power setting nevertheless seemed to work better than the linear case, as reported in ref 18. Very recently, intensive examinations have shown in the study of the generalized Nosé−Hoover equation[22] that we can obtain the BG distribution for the 1HO by only a suitable choice of $\tau(\zeta)$ (i.e., $q = 1$ is retained) if we allow a certain amount of the error or some stiffness of the equation.

3.1.2. One-Dimensional Double-Well. We investigated the 1DW

$$U(x) = D(x^2 - 1)^2 \tag{7}$$

In all 1DW simulations, we used $\Delta t = 5 \times 10^{-4}$. First, we applied the barrier height of $D = 5k_BT$ ($k_B \equiv 1$). Simulation results for the TD using $\tau(\zeta) = 600\zeta$ are exhibited in Figures 3 and 4. Panels a and b in Figure 3 show expectation values, $\langle U \rangle$ and $\langle p^2 \rangle$, calculated by $\overline{U}^{\mathrm{BG},t}$ and $\overline{p^2}^{\mathrm{BG},t}$, respectively, up to $t = 5000$ ($N = 10^7$). Figure 4 shows MDDs at both $N = 5 \times 10^6$ and 10^7 time steps. These simulation values at $N = 10^7$ agreed well with the theoretical values, and the agreement was better at $N = 10^7$ than that at $N = 5 \times 10^6$.

We applied the same potential to the NHC method, using the same conditions in the 1HO simulation except the Δt stated above and the masses Q_1 and Q_2. We tried several values, $Q_1 = Q_2 = 10$, 1, 0.5, 0.2, 0.14, 0.12, 0.1, 0.08, 0.06, 0.05, 0.01, 0.005, and 0.001, and show the MDDs with $Q_1 = Q_2 = 0.1$ for which the error of MDD for x, $\Delta_x(N\Delta t)$, was minimum among those for the above Q_j values at $N = 5 \times 10^6$ time steps (Figure 5a,b). We also exhibited these MDDs at $N = 10^7$ (Figure 5c,d). We noted that for the NHC method better agreement for f_x was not necessarily observed at $N = 10^7$ than that at a shorter period of $N = 5 \times 10^6$. As shown in this result, the evaluation of the simulated BG distributions requires a certain careful treatment, suggesting a concern with the information beyond the instantaneous values of the distribution and a single simulation condition. We will return to this point later.

Note that we used a classical but a general-purpose integration scheme, the 4th-order Runge−Kutta (RK) method, and this may not be the most suitable method for integrating the NHC equation. Discussions of the integration have appeared in, e.g., refs 23 and 24. We examined whether the "conserved quantity"[8] H' was preserved. In the result, $\Delta H'(N) \equiv |H'(N\Delta t) - H'(N_0\Delta t)|/|H'(N_0\Delta t)| \simeq 7 \times 10^{-10}$ for $Q_1 = Q_2 = 0.1$, and $\Delta H'(N) \simeq 8 \times 10^{-7}$ even for the smallest $Q_1 = Q_2 = 0.001$ (the most severe case), both at $N = 10^7$ time steps. These conservations are considered as a justification for our simulations. More sophisticated integration schemes are discussed in ref 24, and the NHC equation with the same potential as that of eq 7 is examined. The simulation conditions for the equation employed in ref 24 were the same as ours except Δt, the time steps N, and $p_{\eta_2}(0)$ (but the total time $N\Delta t = 2500$ was the same). Their results regarding the NHC method indicated that the system became unequilibrated when a high wall was applied. This situation, which is also discussed below in detail, does not contradict our results. We used the RK integrator because we considered the use of an identical integrator against both the TD and the other methods to be ideal for comparison of the equations, and because the RK integrator seems to be a standard for such a purpose, usually being used in fundamental investigations.[6,25] However, for integrating a specific equation, the use of a general-purpose integrator is not necessarily satisfactory for attaining compatibility between accuracy and the computational overhead.[26,27] Furthermore, one must consider abilities such as realizing reversibility and generating accurately the characteristics in a system, e.g., symmetries, or certain features of the time-evolution map for the ODE (the Jacobian of the map has been targeted in non-Hamiltonian systems; see, e.g., ref 24 and the references therein) in the numerical integration. Thus, developing a more efficient integrator for the TD, in view of these issues, is important, particularly if one wants to apply the method to long simulations for large systems.

We applied the potential model with high wall to examine the difference between the TD and the BGD. Figure 6 shows MDDs obtained in the TD simulation with $N = 10^8$ and $\tau(\zeta) = 1400\zeta$ for the barrier-height $D = 10k_BT$. Simulation results agreed well with the theoretical values. We chose $\tau(\zeta) = c\zeta$, and for several values of the parameter c we show the error of MDD, $\Delta_i(t)$, in Figure 7. The errors were small enough in all cases. In addition, we performed simulations for several initial values of $x(0) = 1$, $p(0) = 1$; $x(0) = -1$, $p(0) = 1$; $x(0) = 0.01$, $p(0) = 1$; $x(0) = 0$, $p(0) = 1.01$, as compared with the condition $x(0) = 0$, $p(0) = 1$, used so far. No considerable dependence on the initial values was found, as shown in Figure 8.

We applied the same potential with $D = 10k_BT$ to the NHC method; $\Delta_i(t)$ is shown in Figure 9 for several values of $Q_1 = Q_2$. The unit time size Δt seemed to be in an allowable range, since $\Delta H'(10^8) \simeq 7 \times 10^{-6}$ when $Q_1 = Q_2 = 0.001$ (the most severe case) was applied. To examine the simulation consistency as the necessary condition of the ergodicity, we calculated the distribution density for the thermostat momentum p_{η_j} ($j = 1, 2$) and its total error $\Delta p_{\eta_j}(t) \equiv ||fp_{\eta_j}{}^t - fp_{\eta_j}||_1$, where $fp_{\eta_j}{}^t$ is the simulated density evaluated up to time t and $fp_{\eta_j}(\bullet) \equiv (2\pi k_BTQ_j)^{-1/2} \exp[-(\bullet)^2/2k_BTQ_j]$ is the theoretical one. The behavior of the errors was similar to that of the $\Delta_p(t)$ (Figure 9b), and their values were small, so that $\Delta p_{\eta_j}(5 \times 10^4) \lesssim 2 \times 10^{-2}$ for all the cases in Figure 9, suggesting that the parameters Q_1 and Q_2 were in an appropriate range. This applicability to a wide range of values of the parameters is one of the advantages of the NHC method.

Concerning the distribution for x, however, the error $\Delta_x(t)$ for the NHC did not show a fast decline, but instead it showed oscillating behavior (Figure 9a). For several initial values along with certain fixed Q_j values, similar results were obtained. Now, we show the trajectories of x up to $N = 10^8$ time steps for the

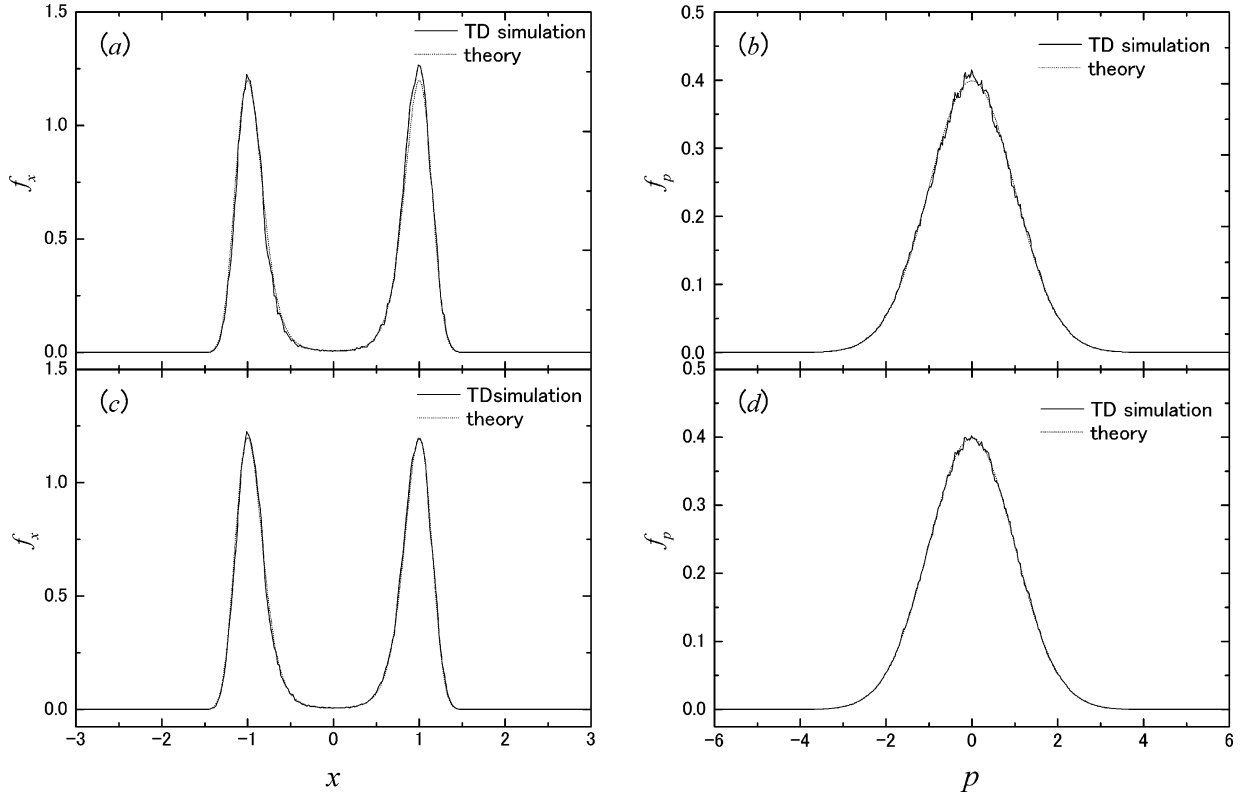

Figure 4. MDD for 1DW with $D = 5k_BT$ for (a) x and (b) p. The solid and dotted lines indicate simulation results obtained by TD at $N = 5 \times 10^6$ time steps and the theoretical values, respectively. Simulation results at $N = 10^7$ for x and p are in (c) and (d), respectively.

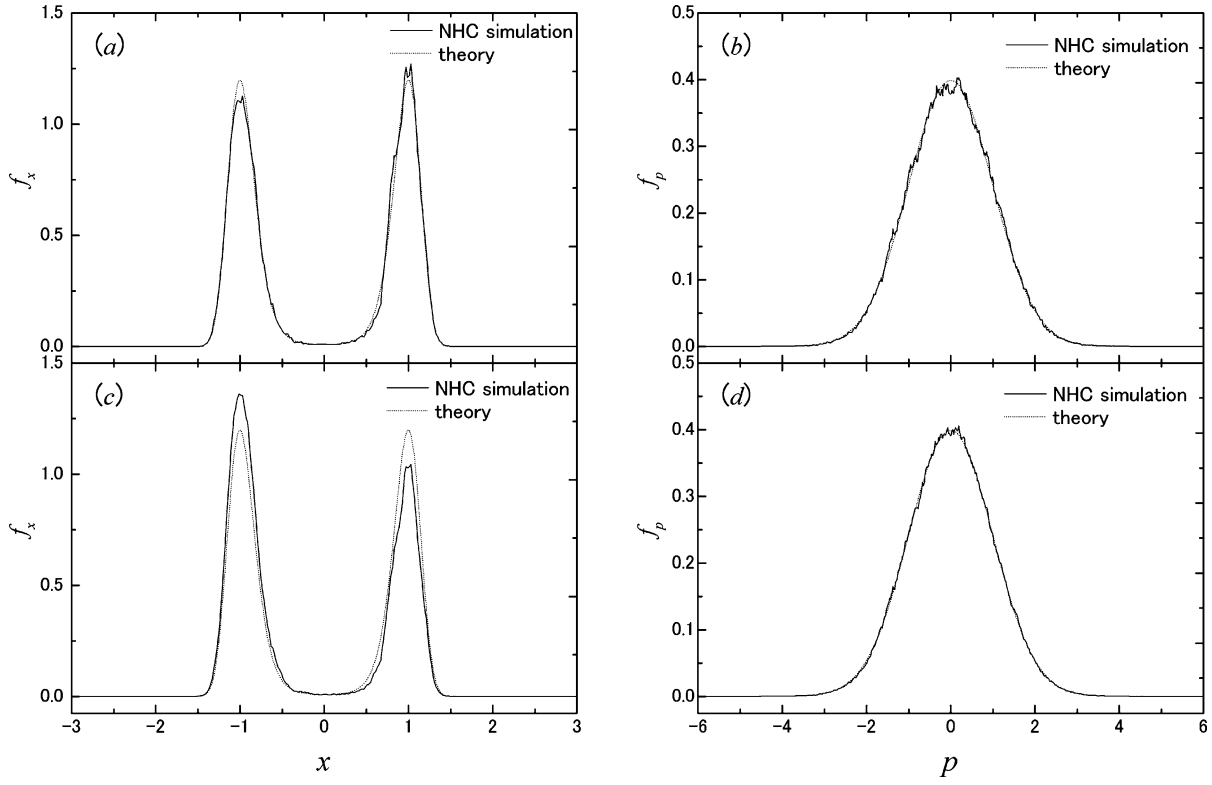

Figure 5. MDD for 1DW with $D = 5k_BT$ for (a) x and (b) p. The solid and dotted lines indicate simulation results obtained by NHC at $N = 5 \times 10^6$ time steps and the theoretical values, respectively. Simulation results at $N = 10^7$ for x and p are in (c) and (d), respectively.

TD (the case of $c = 1400$ in Figure 7) and the NHC [the case of $Q_1 = 0.05$ in Figure 9; this Q_1 value resulted in a minimum of the error $\Delta_x(t)$ at $t = 10^8\Delta t$ among those indicated in Figure 9a] in Figure 10, panels a and b, respectively. The behavior of $\Delta_x(t)$ in Figure 9a can be explained based on the observation of transitions (a jump from one potential-well to the other) like those shown in Figure 10b. First, the constancy of $\Delta_x(t) \simeq 1$ until $t = t_l \simeq 1.4 \times 10^4$ in the case of $Q_1 = 0.05$ in Figure 9a corresponded to the sojourn of $x(t)$ in one well until $t = t_l$, shown in Figure 10b (analytical discussion on such a correspondence

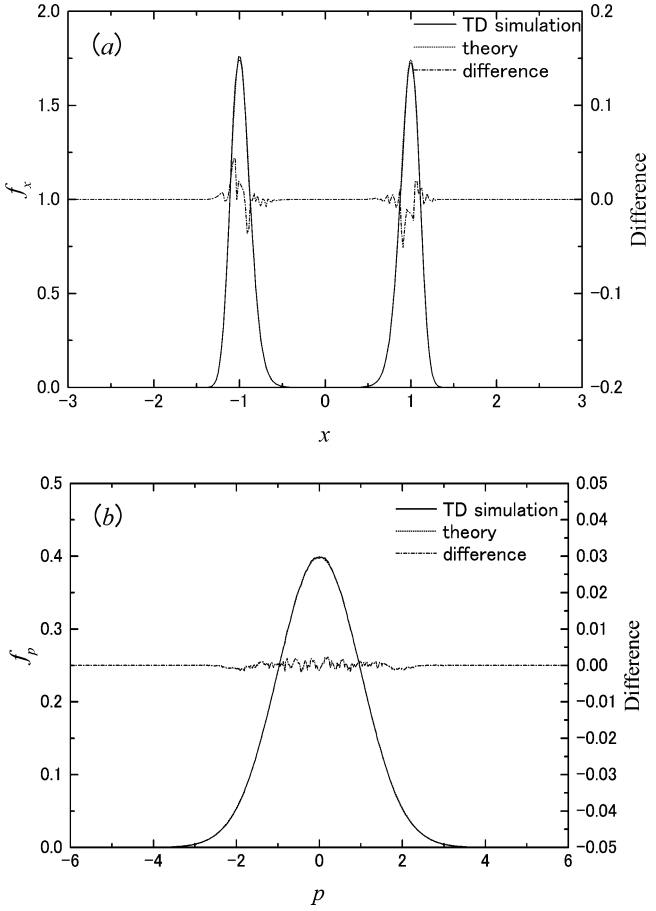

Figure 6. MDD for 1DW with $D = 10k_BT$ for (a) x and (b) p. Simulation results obtained by TD, the theoretical values, and their differences on enlarged scales are shown.

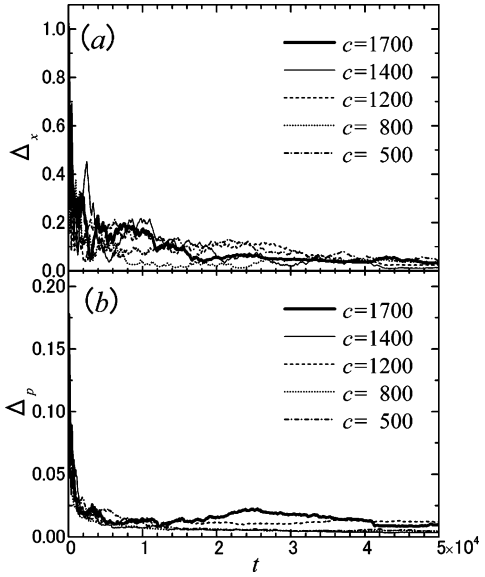

Figure 7. The total error of MDD, obtained by TD, for 1DW with $D = 10k_BT$. The errors vs time t for (a) x and (b) p are shown for indicated values of the parameter c.

in a general sense is also possible under some assumptions). Second, the increase in the $\Delta_x(t)$ oscillation occurred (i) after the transition that happened while $\Delta_x(t)$ was decreasing (see the transition at $t \simeq 2 \times 10^4$ in Figure 10b) or (ii) when a sojourn in one well continued for a long time (e.g., $2 \times 10^4 \lesssim t \lesssim 3.6 \times 10^4$ for the case of $Q_1 = 0.001$ in Figure 9a). When the transitions are observed statistically fully, so as to realize a

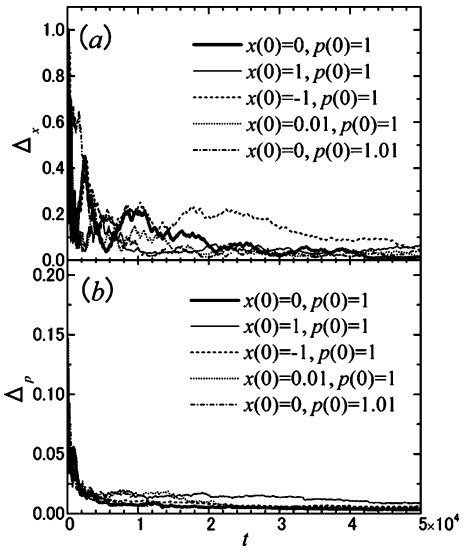

Figure 8. The total error of MDD, obtained by TD, for 1DW with $D = 10k_BT$. The errors vs time t for (a) x and (b) p are shown for indicated initial values.

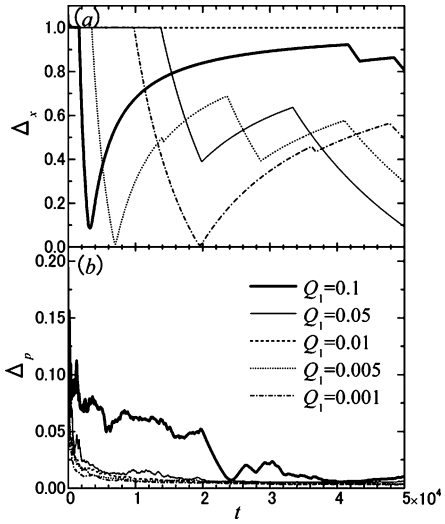

Figure 9. The total error of MDD, obtained by NHC, for 1DW with $D = 10k_BT$. The errors vs time t for (a) x and (b) p are shown for indicated values of the parameter Q_1 ($=Q_2$).

distribution that is robust enough against the above "fluctuations" of condition i or ii, the oscillation will become small and will not be prominent.

We thus examined the validity of the number of transitions observed in these BGD simulations from a theoretical view. We employed the transition-state theory (TST) approximation[28] to give a rough estimation of the number of transitions. According to this, the transition probability from the state $x < 0$ to the state $x > 0$ in one-dimensional BGD is estimated as $\Delta t\langle\delta(x)\dot{x}\Theta(\dot{x})\rangle/\langle\Theta(-x)\rangle$, where δ is the Dirac delta function and Θ is the Heaviside step function. Hence, for the $D = 10k_BT$ model in the NHC simulations, the transition probability between the two states is $P_{\mathrm{Trnst}} \equiv 2\Delta t\langle\delta(x)\dot{x}\Theta(\dot{x})\rangle/\langle\Theta(-x)\rangle = 4f_x(0)\langle p\Theta(p)\rangle\Delta t \simeq 6.3 \times 10^{-8}$. Thus, the number of transitions during $N = 10^8$ time steps is $N \times P_{\mathrm{Trnst}} \simeq 6$, supporting the preceding simulation results. The feature of the transitions in the above NHC simulations was thereby considered to be a faithful realization of the BGD.

In contrast, quick transitions were generated in the TD. There were 736 transitions during the TD simulation shown in Figure 10a. The average number of transitions among the five TD

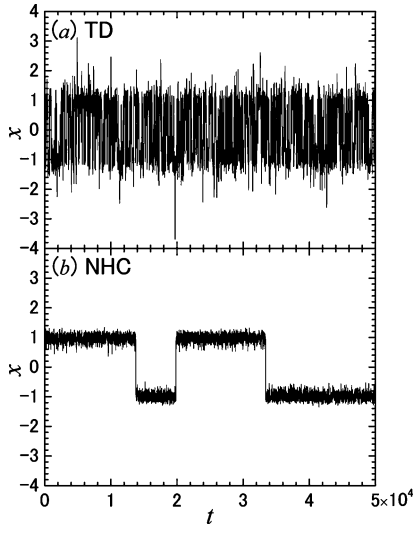

Figure 10. Trajectories of x for 1DW with $D = 10k_BT$ for (a) TD and (b) NHC.

simulations exhibited in Figure 8 was 767. Such a quick transition in the TD provides a basis for a fast convergence of the BG distribution and for statistically stable results.

To further examine the barrier-jumping abilities, we applied the current TD method to the model with $D = 100k_BT$ and obtained the MDDs for $N = 10^8$ and $\tau(\zeta) = 1700\zeta$ (Figure 11). Although the error in f_p remained around p where change of the distribution value is the most rapid, the simulation results and theoretical values agreed within small differences. This supports a high potentiality for sampling using the TD method.

In the cases of $D = 5k_BT$ and $100k_BT$ in the TD simulations, we showed the results concerning a specified value of c in $\tau(\zeta) = c\zeta$. We have also tried several values of c around it in both cases. In the case of $D = 5k_BT$, the results of the errors of the MDDs for $c = 100$, 500, and 1000 were not significantly different from those for $c = 600$ shown above. We note, however, that all values of c did not always lead to the same results. For example, for a relatively small value of c in $D = 100k_BT$, there was a case in which the MDD error remained at a positive value within the $N = 10^8$ time steps investigated. In comparison, a very high value of c grows stiffness in the ODE. From our experience, an appropriate intermediate value would be needed for the setting (cf. ref 1).

So far, we have discussed the NHC method from the view that the method is used for direct sampling of the BG distribution, as treated in the original proposal. However, it is true that the NHC also provides a base for the development of a new phase-space dynamics, besides the original aspect as the BGD. For example, recently, the NHC method has been successfully applied to generate a certain transformed BG distribution, giving enhanced conformational sampling.[29] Also the TD itself is based on the NH method, which is the BGD providing a typical phase-space dynamics; and alternatively, the TD based on the NHC method can be considered.

3.2. Alanine Tripeptide. The free energy landscape of the alanine tripeptide system has been studied intensively.[30−32] We thus applied our protocol to this peptide in vacuo, as a benchmark test. The potential function U was provided by the C96 force field for the AMBER of the all-atom version,[33,34] consisting of interactions for bond, angle, dihedral, and the nonbonded van der Waals and Coulomb. The N and C termini of the peptide were capped with acetyl and N-methyl groups, respectively. An extended conformation was taken as the initial structure. The parameters for the TD were $q = 1.0105$ and $T' = 200$ K. This value of q was the order of magnitude of $1 + 1/n$, where n is the number of degrees of freedom for the system. We used $U + E_0$ rather than U itself, where $E_0 \equiv -\tilde{U}_{\text{inf}} - k_BT'/(q-1) + \epsilon$, $\tilde{U}_{\text{inf}}$ being a candidate of the infimum of U. If $\epsilon > \tilde{U}_{\text{inf}} - U_{\text{inf}}$, where U_{inf} is the true infimum, then $U + E_0 > k_BT'/(1-q)$, ensuring that the density of the Tsallis distribution of eq 1 is well-defined. The constant $\tilde{U}_{\text{inf}}$ can be practically determined by a certain presimulation on the BGD at a low temperature. We set $\tilde{U}_{\text{inf}} = -25$ kcal/mol, which was the minimum value of the potential energy obtained in the presimulation at 50 K, and we set $\epsilon = 4$ kcal/mol. After this, we performed the TD simulation during 2.5×10^7 time steps using $\Delta t = 0.1$ fs. The density for ζ was set to be $\rho_z(\zeta) \equiv \exp(-c\zeta^2)$ with $c = 10^4$ (g/mol)$^{-2}$ Å^{-4} fs^2. The simulations were performed by the program PRESTO[35] with a modification for the TD.

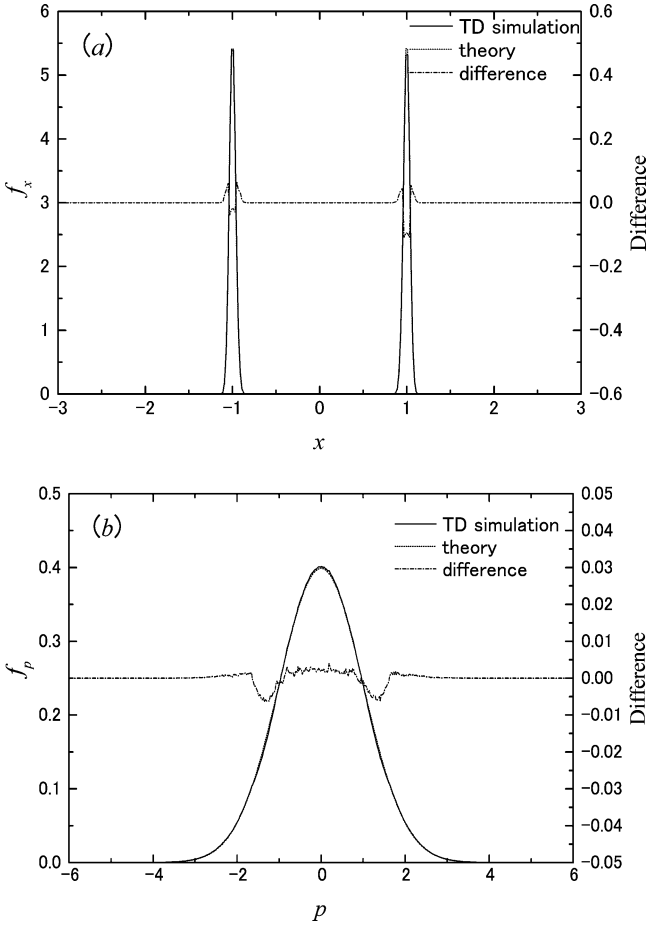

Figure 11. MDD for 1DW with $D = 100k_BT$ for (a) x and (b) p. Simulation results obtained by TD, the theoretical values, and their differences on enlarged scales are shown.

Figure 12 shows the potential energy distribution $P(u)$, evaluated by the rate such that $u - \Delta/2 \le U(x(t)) < u + \Delta/2$ during the simulation by the TD, and those for the BG distributions at temperature $T = 150$, 300, 900, and 1500 K produced by the reweighting formula of eq 4. The BG distribution reweighted by the TD and that obtained by the conventional BGD were located in a similar region, for these temperatures. Compared with the BG distributions, the distribution sampled by the TD covered a significantly wide region in the potential energy space, viz., the space imaged by a map U. As exhibited in Figure 12, the BG distribution at 300 K brought by the TD agreed with that provided by the conventional MCMD method, which covered the region from that for the

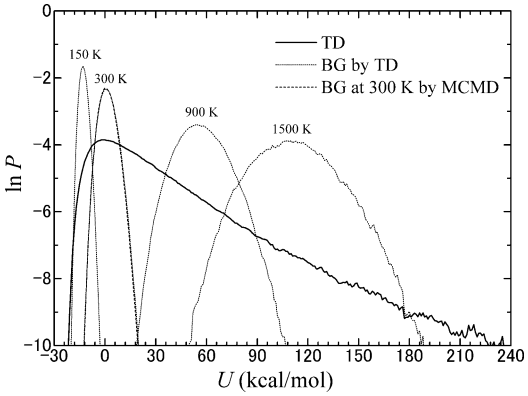

Figure 12. Potential energy distribution $P(U)$ for the Ac-Ala-Ala-NMe system. Simulation results by TD are shown by a solid line. Dotted lines show results for the BG distribution at temperatures of 150, 300, 900, and 1500 K from left to right, obtained by the reweighting in TD simulation. The dashed line shows the BG distribution at 300 K obtained by the MCMD simulation.

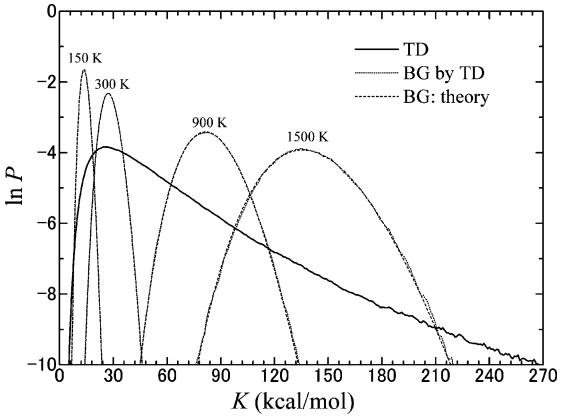

Figure 13. Kinetic energy distribution $P(K)$ for the Ac-Ala-Ala-NMe system. Simulation results by TD are shown by a solid line. Dotted lines show results for the BG distribution at temperatures of 150, 300, 900, and 1500 K from left to right, obtained by the reweighting in TD simulation; dashed lines show respectively those exact distributions.

BG distribution at 700 K to that at 300 K. This suggests the validity of the sampling in the potential energy space by the TD. In Figure 13, we showed a kinetic energy distribution obtained in a way similar to that described above in the TD simulation, the reweighting results at the four temperatures, and the theoretical values of those BG distributions. The reweighting results and the theoretical values agreed well, indicating that the TD sampled the kinetic energy space with sufficient accuracy. To further examine sampling features by another map, we calculated the O_1-H_4 distance $d_{1,4}$, which can measure the difference between the closed and open reverse-turn structures.[30,31] Figure 14 shows the potential of mean force for the BG distribution at $T = 300$ K for $d_{1,4}$, $-k_BT \ln P(d_{1,4})$, where the rate $P(d_{1,4})$ was obtained from the reweighting procedure for the TD. Minima at about 2, 7, and 9 Å, corresponding to each characteristic structure,[32] were observed. These are consistent with the previous simulations by the conventional MCMD method with the same force field.[32]

For a parameter setting of c in $\rho_z(\zeta)$, we have also run simulations using $c = 10$, 10^2, 10^3, and 10^5 (g/mol)$^{-2}$ Å^{-4} fs^2. The potential energy distributions and kinetic energy distributions were essentially the same as those shown in Figures 12 and 13, respectively, although some difference was admitted in a region corresponding to rare events. Regarding q and E_0 (or ϵ), a large system requires that one set appropriate values

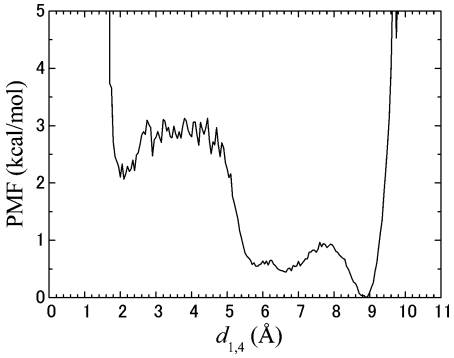

Figure 14. Potential of mean force (PMF) for the O_1-H_4 distance $d_{1,4}$ for the Ac-Ala-Ala-NMe system in the BG distribution at 300 K, obtained by the reweighting in TD simulation.

for these parameters for effective sampling. In this study, we fine-tuned them by an ad hoc manner to reach the sampling covering the desired region in the potential energy space. As the number of degrees of freedom for the system increases, however, such a naive procedure will be time consuming. Thus, a systematic way to determine those parameters for effective sampling is an issue for further developing the present approach in the sampling problem of large systems.

4. Conclusions

We performed numerical examinations of the ability of the TD combined with a reweighting technique to produce the BG distributions, comparing the results with those of other, direct approaches. In 1HO and 1DW systems, we have obtained promising results. For 1HO, against the unwilling nonergodic behavior of the system, the BG distributions were produced as successfully as when the NHC method was employed. In 1DW systems, the difference between the TD and the NHC method as BGD was observed in the barrier crossing feature. The TD has provided sufficient transitions among the wells even for high-energy walls during the simulation time examined, and the simulations generated correct BG distributions. We have shown in the alanine tripeptide system that the TD sampled the potential energy region widely from low to high, compared with those for the BGD, and produced the correct kinetic energy BG distributions.

Future development allowing application to larger systems will be facilitated if a systematic method is constructed to determine the parameters q, T', and E_0 for effective sampling. An efficient numerical integrator will be of great value for large-scale simulations.

Acknowledgment. We thank Professor Akinori Kidera for his helpful comments. We also thank Yukihisa Watanabe, Yoshiaki Mikami, and Takashi Kurosawa for their kind help in performing the simulations. The New Energy and Industrial Technology Development Organization is acknowledged for its financial support of this study.

References and Notes

(1) Nosé, S. *Prog. Theor. Phys. Suppl.* **1991**, *103*, 1.
(2) Nosé, S. *J. Chem. Phys.* **1984**, *81*, 511.
(3) Hoover, W. G. *Phys. Rev. A* **1985**, *31*, 1695.
(4) Hoover W. G.; Holian, B. L. *Phys. Lett. A* **1996**, *211*, 253.
(5) Sergi A.; Ferrario, M. *Phys. Rev. E* **2001**, *64*, 056125.
(6) (a) Hoover, Wm. G. *Computational Statistical Mechanics*; Elsevier: New York, 1991. (b) Hoover, Wm. G. *Time Reversibility, Computer Simulation, and Chaos*; World Scientific: Singapore, 1999.
(7) Posch, H. A.; Hoover, W. G.; Vesely, F. J. *Phys. Rev. A* **1986**, *33*, 4253.

(8) Martyna, G. J.; Klein, M. L.; Tuckerman, M. *J. Chem. Phys.* **1992**, *97*, 2635.
(9) Cheng, A.; Merz, K. M., Jr. *J. Phys. Chem.* **1996**, *100*, 1927.
(10) Brańka, A. C. *Phys. Rev. E* **2000**, *61*, 4769.
(11) Kusnezov, D.; Bulgac, A.; Bauer, W. *Ann. Phys.* **1990**, *204*, 155.
(12) L'Heureux, I.; Hamilton, I. *Phys. Rev. E* **1993**, *47*, 1411.
(13) Ferrenberg A. M.; Swendsen, R. H. *Phys. Rev. Lett.* **1988**, *61*, 2635.
(14) Nakajima, N.; Nakamura, H.; Kidera, A. *J. Phys. Chem. B* **1997**, *101*, 817.
(15) Tsallis, C. *J. Stat. Phys.* **1988**, *52*, 479.
(16) Tsallis, C. *Braz. J. Phys.* **1999**, *29*, 1.
(17) Plastino, A. R.; Anteneodo, C. *Ann. Phys.* **1997**, *255*, 250.
(18) Fukuda I.; Nakamura, H. *Phys. Rev. E* **2002**, *65*, 026105.
(19) Andrade, J. S., Jr.; Almeida, M. P.; Moreira, A. A.; Farias, G. A. *Phys. Rev. E* **2002**, *65*, 036121.
(20) Winkler, R. G. *Phys. Rev. A* **1992**, *45*, 2250.
(21) Tsallis, C.; Mendes, R. S.; Plastino, A. R. *Physica A (Amsterdam)* **1998**, *261*, 534.
(22) Brańka, A. C.; Kowalik, M.; Wojciechowski, K. W. *J. Chem. Phys.* **2003**, *119*, 1929.
(23) Martyna, G. J.; Tuckerman, M. E.; Tobias, D. J.; Klein, M. L. *Mol. Phys.* **1996**, *87*, 1117.
(24) Liu, Y.; Tuckerman, M. E. *J. Chem. Phys.* **2000**, *112*, 1685.
(25) Splott, J. C. *Phys. Rev. E* **1994**, *50*, R647.
(26) Zhang, F. *J. Chem. Phys.* **1997**, *106*, 6102.
(27) Ishida H.; Kidera, A. *J. Chem. Phys.* **1998**, *109*, 3276.
(28) Hänggi, P.; Talkner, P.; Borkovec, M. *Rev. Mod. Phys.* **1990**, *62*, 251.
(29) Zhu, Z.; Tuckerman, M. E.; Samuelson, S. O.; Martyna, G. J. *Phys. Rev. Lett.* **2002**, *88*, 100201.
(30) Tobias, D. J.; Sneddon, S. F.; Brooks, C. L., III *J. Mol. Biol.* **1990**, *216*, 783.
(31) Beglov, D.; Roux, B. *Biopolymers* **1995**, *35*, 171.
(32) Ono, S.; Nakajima, N.; Higo, J.; Nakamura, H. *J. Comput. Chem.* **2000**, *21*, 748.
(33) Cornell, W. D.; Cieplak, P.; Bayly, C. I.; Gould, I. R.; Merz, K. M., Jr.; Ferguson, D. M.; Spellmeyer, D. C.; Fox, T.; Caldwell, J. W.; Kollman, P. A. *J. Am. Chem. Soc.* **1995**, *117*, 5179.
(34) Kollman, P.; Dixon, R.; Cornell, W.; Fox, T.; Chipot, C.; Pohorille, A. In *Computer Simulation of Biomolecular Systems*; van Gunsteren, W. F., Weiner, P. K., Wilkinson, A. J., Eds.; Kluwer: Dordrecht, The Netherlands, 1997; Vol. 3, pp 83−96.
(35) Morikami, K.; Nakai, T.; Kidera, A.; Saito, M.; Nakamura, H. *J. Comput. Chem.* **1992**, *16*, 243.